Journal of Colloid and Interface Science 370 (2012) 170–175

Contents lists available at SciVerse ScienceDirect

Journal of Colloid and Interface Science

www.elsevier.com/locate/jcis

Coverage-dependent morphology of PEGylated lysozyme layers adsorbed on silica

Sheetal S. Pai [a,b], Frank Heinrich [d,e], Adam L. Canady [a,b], Todd M. Przybycien [a,b,c,*], Robert D. Tilton [a,b,c,*]

[a] Center for Complex Fluids Engineering, Carnegie Mellon University, Pittsburgh, PA 15213, USA
[b] Department of Chemical Engineering, Carnegie Mellon University, Pittsburgh, PA 15213, USA
[c] Department of Biomedical Engineering, Carnegie Mellon University, Pittsburgh, PA 15213, USA
[d] Department of Physics, Carnegie Mellon University, Pittsburgh, PA 15213, USA
[e] NIST Center for Neutron Research, National Institute of Standards and Technology, Gaithersburg, MD 20899, USA

ARTICLE INFO

Article history:
Received 28 September 2011
Accepted 22 December 2011
Available online 4 January 2012

Keywords:
Poly(ethylene glycol)
Lysozyme
PEGylation
Neutron reflectivity
Protein adsorption
Polymer conformation
Silica

ABSTRACT

Neutron reflection was used to characterize the adsorbed layer structure for lysozyme conjugated at the N-terminus with a single perdeuterated methoxy poly(ethylene glycol) (PEG) chain at the silica/water interface. Adsorbed layers were produced with two different surface concentrations corresponding to opposite sides of a pronounced transition in the adsorption isotherm for mono-PEGylated lysozyme. The transition was previously ascribed, on the basis of less direct characterization by normal force measurements, to a change in the distribution of the conjugated PEG chain segments in the interfacial region in response to lateral repulsions (S.M. Daly, T.M. Przybycien, R.D. Tilton, Langmuir 21 (2005) 1328–1337). Neutron reflectivity was measured for both surface concentrations using three different sets of neutron scattering length density contrast conditions, and models for the distribution of PEG and lysozyme content in the layers were obtained by simultaneous regression of all contrast condition data sets. This analysis indicated that the surface proximal volume is occupied almost equally by PEG and lysozyme at the low surface concentration, while at the higher surface concentration PEG is preferentially shifted away from the surface, with all lysozyme remaining in the surface proximal region. The distal regions of the high surface concentration layer contain only PEG, consistent with the previous interpretation of normal force measurements.

1. Introduction

Adsorption to the solid/liquid interface is relevant to the chromatographic purification of poly(ethylene glycol)-conjugated proteins, i.e. "PEGylated proteins", a growing class of modern pharmaceutical agents [1]. We previously reported evidence based on optical reflectometry, total internal reflection fluorescence spectroscopy, and atomic force microscopy (AFM) normal force measurements that poly(ethylene glycol) (PEG) chains conjugated to lysozyme (mono-PEG-lysozyme) assume a mushroom-like conformation when mono-PEG-lysozyme is adsorbed to a silica surface at high surface coverage, whereas the conjugated PEG chains made more extensive contact with the surface at low coverage [2]. While unmodified lysozyme adsorbed above a threshold surface coverage assumes a preferred orientation that maximizes electrostatic attraction to the oppositely charged silica surface and minimizes lateral electrostatic repulsion [3–5], the mono-PEG-lysozyme conjugate reorientation to a lysozyme-anchored mushroom configuration at high coverage maximizes lysozyme attraction to the oppositely charged silica surface and minimizes steric repulsion among conjugated PEG chains [2]. These lateral interaction-induced morphological re-arrangements manifest as breaks in the adsorption isotherms for unmodified lysozyme and mono-PEG-lysozyme as shown in Fig. 1.

The locus of PEG chain attachment is an important determinant of conjugate adsorption behavior. Because the PEGylation approach we have used is based on an aldehyde-activated PEG chemistry and is conducted at acidic pH, conjugation occurred primarily at the N-terminal lysine residue. This residue is located in contact with the surface in the preferred orientation of unmodified lysozyme when it adsorbs to silica near neutral pH [2]. The N-terminal PEG conjugation forces the lysozyme portion of the PEGylated protein conjugate to adopt a less energetically favorable orientation relative to the surface as evidenced by the smaller initial slope of the mono-PEG lysozyme adsorption isotherm (Fig. 1) and the greater adsorption reversibility relative to unmodified lysozyme [2]. The overall destabilizing effect of steric repulsions among conjugated PEG chains in the adsorbed layer may also contribute to the increased adsorption reversibility of the conjugates.

The main evidence in the previous work for the transition from a relatively flat configuration of the PEG portion of the conjugates

* Corresponding authors. Address: Department of Chemical Engineering, Carnegie Mellon University, Pittsburgh, PA 15213, USA.
E-mail addresses: todd@andrew.cmu.edu (T.M. Przybycien), tilton@andrew.cmu.edu (R.D. Tilton).

0021-9797/$ - see front matter © 2012 Elsevier Inc. All rights reserved.
doi:10.1016/j.jcis.2011.12.065

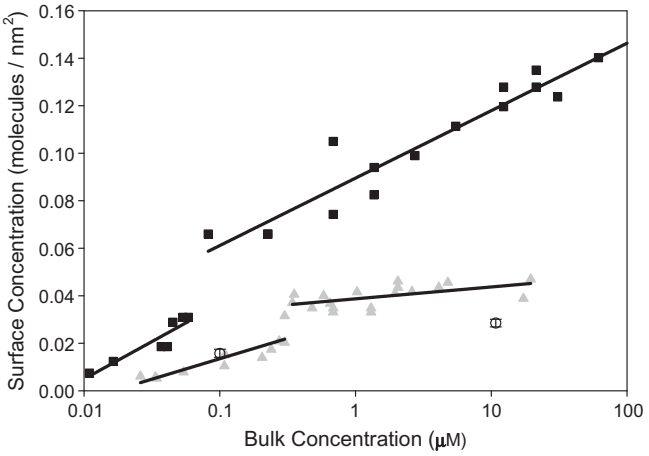

Fig. 1. Adsorption isotherms of unmodified lysozyme (filled squares) and mono-PEG-lysozyme (gray-filled triangles) in 5 mmol/L, pH 7.4 TEA buffer on silica as determined previously by optical reflectometry [2]. The lines are linear regressions of the corresponding data. Surface concentrations of mono-PEG-lysozyme on silica at low and high bulk concentrations as determined by neutron reflectivity are also shown (open circles) along with 95% confidence limits.

to a mushroom-like configuration, where end-grafted PEG chains extend outward into solution with little surface contact, but with little or none of the brush-like stretching that would be caused by steric repulsions at higher surface densities, came from analysis of the average excluded surface area per conjugate calculated via the adsorption isotherm, and also from AFM normal force measurements. The latter indicated that the repulsion between opposing adsorbed layers could not be distinguished from the electrostatic double layer repulsion at low coverage, while a steric repulsion was evident in the long-range surface normal force at high coverage. The evidence for the change in PEG distribution is strong, but the methods used could not directly test the proposed anchored-mushroom configurational model. Although considered less likely, the possibility remained that the conjugates were anchored by the PEG chains (which are surface active on silica), leaving a compressible layer consisting of dangling lysozyme molecules tethered to the surface via PEG chains.

Here we exploited the molecular length scale resolution of neutron reflection in combination with scattering length density contrast matching [6] to confirm a transition in the structure of adsorbed mono-PEG-lysozyme layers as the surface coverage exceeds the break in the adsorption isotherm and to validate the proposed lysozyme-anchored mushroom model at high surface coverage. The layer model was tested by simultaneous fitting of reflectivity data for three distinct combinations of water isotopic contrasts to a two-sublayer model for the adsorbed mono-PEG-lysozyme layer. These new findings confirm the difference in PEG configuration at low and high coverage, from a layer with both PEG and lysozyme contacting the surface at low coverage to a layer where PEG is preferentially displaced away from the surface at higher coverage.

2. Materials and methods

2.1. Materials

Chicken egg lysozyme (Sigma–Aldrich Company, cat. No. L-6876) was conjugated with 22 kDa perdeuterated methoxy-poly(ethylene glycol) propionaldehyde (*d*PEG) using methods described previously [2,7]. Details of the synthesis of *d*PEG were also described previously [8]. After size exclusion chromatography-based fractionation of the reaction products according to the number of *d*PEG chains per conjugate, the mono-*d*PEG-lysozyme was buffer exchanged into pH 7.4, 5 mmol/L triethanolamine hydrochloride (TEA; Sigma–Aldrich Company) solution, the same buffer used in the prior adsorption studies [2,5]. The two polished silicon wafers used in this work (5 Å RMS roughness; orientation [1 0 0], n-type Si:P doped) had a native oxide surface layer and were obtained from El-Cat Inc., Waldwick NJ, and cleaned with NoChromix (Sigma–Aldrich Company), 6 mol/L HCl (Fisher Scientific), and 10 mmol/L NaOH (Sigma–Aldrich Company) according to the protocol described previously [2,7]. This cleaning procedure leaves the oxide surface negatively charged with a surface charge density of approximately one charge per 800 nm^2 at neutral pH, as calculated from zeta potential measurements [4].

2.2. Neutron reflection experiments

Neutron reflection measurements were carried out at the NG-1 ANDR, Advanced Neutron Diffractometer/Reflectometer at NIST[9] Center for Neutron Research (NCNR), using the NCNR flow cell [10]. Measurements using three different bulk water compositions, 100% D_2O, 100% H_2O, and "CM4" (a 2:1 D_2O:H_2O mixture), provided for different scattering length density contrasts with the lysozyme and *d*PEG portions of the conjugates. Data were collected as the reflected intensity versus the angle of reflection, $I(\theta)$, and expressed as the reflectivity $R(Q_z)$, defined as $R(Q_z) = I(Q_z)/I_0$, with the momentum transfer Q_z defined as $(4\pi/\lambda)\sin(\theta)$ with a neutron wavelength of $\lambda = 5.00 \pm 0.05$ Å. For each contrast condition, neutron counting proceeded for at least 7 h. Bulk solution neutron scattering length density (*nSLD*) values were determined from scattering profiles collected in the absence of conjugate.

Solutions of 10.8 μmol/L or 0.1 μmol/L mono-*d*PEG-lysozyme were selected to provide surface concentrations well above or well below the adsorption transition, respectively [2]. All samples that were originally lyophilized from solution in 5 mmol/L TEA, pH 7.4 buffer were re-suspended into a volume of the appropriate aqueous solvent to recover a 5 mmol/L TEA, pH 7.4 solution. (Circular dichroism indicated that neither PEGylation nor lyophilization significantly perturbed the lysozyme secondary structure.) The high and low bulk concentration experiments were conducted on separate silicon wafer substrates. The use of a flow cell allowed all buffer rinses, protein adsorption steps and reflectivity measurements to be done *in situ* with no drying steps. After equilibrating the appropriate substrate with 100% D_2O, solutions of mono-*d*PEG-lysozyme at 10.8 μmol/L or 0.1 μmol/L in 100% D_2O were introduced to the sample cell and allowed to incubate for 9 h. Neutron counting commenced 30 min after introducing the mono-*d*PEG-lysozyme solution. The substrate was then rinsed and incubated with 3 mL solutions (2.5 flowcell volumes) of mono-*d*PEG-lysozyme at 10.8 μmol/L or 0.1 μmol/L in CM4 for 7 h. Finally, the sample cell was rinsed and incubated with 3 mL solutions of mono-*d*PEG-lysozyme at 10.8 μmol/L or 0.1 μmol/L in 100% H_2O for 7 h. All experiments were conducted at room temperature.

2.3. Data analysis

Neutron reflection data for each sample were analyzed simultaneously for the three different neutron scattering length density contrast conditions. The *nSLD* model applied is a box model [11] using two sublayers to represent the density distribution for the PEG-protein conjugate in the adsorbed layer; the boxes comprised: bulk Si/SiO_2 layer/sublayer 1/sublayer 2/bulk solution. Each of the two sublayers was allowed to be occupied by solvent, lysozyme and *d*PEG, with concentrations expressed as volume fractions. The model regression was constrained so that the total volumes (amounts) of lysozyme and *d*PEG in the two layers corresponded to a 1:1 molar ratio of 22 kDa *d*PEG chains and 14.3 kDa lysozyme

molecules as expected for the mono-*d*PEG-lysozyme conjugate. Table 1 contains the molecular volumes [12], neutron scattering lengths (*nSL*) [13] and neutron scattering length densities (*nSLD*) calculated for use in adsorbed layer model fitting. The experimental background reflectivity was measured and subtracted from the raw reflectivity data; the associated errors are reflected by the error bars. A simultaneous, weighted non-linear least squares fit [14] of the neutron reflection profiles for four cases (silicon wafer in D_2O without conjugate; silicon wafer in D_2O, CM4 and H_2O with conjugate) was performed for both the high and low conjugate concentration cases; fitting weights were given by the uncertainties associated with the individual data points. Note that all uncertainties in values reported in the text, tables and figures are 95% confidence limits unless otherwise noted.

3. Results and discussion

Table 2 lists all experimental conditions and the fitted bulk solution neutron scattering length densities. All measurements of adsorbed mono-*d*PEG-lysozyme were conducted with the conjugated protein solution present in the flowcell to maintain steady state adsorption/desorption during the measurements.

Experimental reflectivity curves with simultaneous best fits for the high concentration case (10.8 μmol/L mono-*d*PEG-lysozyme) and low concentration case (0.1 μmol/L mono-*d*PEG-lysozyme) are shown in Figs. 2 and 3, respectively. Insets illustrate the 95% confidence envelopes from Monte Carlo simulations of the scattering length density profiles [15].

Results from the applied box model are listed in Table 3, including the chi-squared values and corresponding *p*-values representing goodness of fit. The overall model fits had high statistical significance in both cases. The oxide layer thicknesses are similar but not identical for the two concentrations because different wafers were used for each measurement. The overall mono-*d*PEG-lysozyme surface concentrations and the distribution of lysozyme and PEG in the layer were different at high and low bulk concentrations as expected. For the high concentration 10.8 μmol/L case, lysozyme is found only in the surface proximal sublayer 1, which has a thickness of about 3 nm, consistent with the $3 \times 3 \times 4.5$ nm X-ray crystallographic dimensions of chicken egg lysozyme (Protein Data Bank file 4LYZ) [16]. The low concentration case also indicates that the thickness of the proximal sublayer is similar to the dimensions of lysozyme but slightly smaller; the larger uncertainty in this case reflects the lower surface coverage and the corresponding reduced contrast with the adjacent layers.

The surface concentrations of lysozyme and/or PEG in each sublayer that correspond to the layer thicknesses and component volume fractions are presented in Table 4 for both high and low bulk concentration conditions. The statistical distributions of local sublayer surface concentrations $\Gamma_{i,j}$ for species j in sublayer i were calculated as $\Gamma_{i,j} = \phi_{i,j} d_i / V_j$ using the sets of species volume fractions $\phi_{i,j}$ and sublayer thicknesses d_i generated in the individual Monte Carlo iterations with the corresponding species molecular volumes V_j reported in Table 1. The statistical distributions for the total surface concentrations were similarly computed as the sum of the sublayer surface concentrations, $\Gamma_j = \Gamma_{1,j} + \Gamma_{2,j}$. The averages of all calculated surface concentrations are reported in Table 4 along with the 95% confidence limits of the distributions.

Table 1
Molecular properties used for *d*PEG and lysozyme species in fitting neutron reflection data.

	Perdeuterated PEG	Lysozyme
Volume, V_j (Å^3)	28000[a]	13960[b]
nSL	4.580×10^{-4} Å per mono-mer	3.254×10^{-2} Å protonated; 5.920×10^{-2} Å exchangeable protons exchanged to deuterium
nSLD	7.63×10^{-6} Å^{-2}	1.847×10^{-6} Å^{-2} protonated; 3.360×10^{-6} Å^{-2} exchangeable protons exchanged to deuterium

[a] Based on measured molecular weight of 22,000 Da, corresponding to 461 repeat units using 48.08 Da/repeat unit and 60 Å^3/repeat unit.
[b] From amino acid sequence [12].

Table 2
Experimental conditions for neutron reflectivity experiments.

Test Surface	Solvent	Bulk solution *nSLD*[a]
Bare silicon wafer #1	D_2O	$6.30^{+0.01}_{-0.01}$
Silicon wafer #1 in contact with 10.8 μmol/L mono-*d*PEG-lysozyme	D_2O	$6.27^{+0.01}_{-0.01}$
	CM4	$3.91^{+0.01}_{-0.01}$
	H_2O	$-0.55^{+0.06}_{-0.01}$
Bare silicon wafer #2	D_2O	$6.32^{+0.01}_{-0.01}$
Silicon wafer #2 in contact with 0.1 μmol/L mono-*d*PEG-lysozyme	D_2O	$6.33^{+0.01}_{-0.01}$
	CM4	$4.05^{+0.01}_{-0.01}$
	H_2O	$-0.35^{+0.05}_{-0.05}$

[a] Bulk *nSLD* values (10^{-6} Å^{-2}) were determined by neutron reflection data fitting. Error limits indicate upper and lower bounds at 95% confidence.

The overall surface concentration, simply the sum of the number of adsorbed molecules per unit area in each sublayer, was $0.0285^{+0.0016}_{-0.0016}$ molecules/nm^2 for the high bulk concentration case and $0.0157^{+0.0018}_{-0.0016}$ molecule/nm^2 for the low concentration case. We previously reported surface concentrations determined by optical reflectometry and analyzed using a single box optical model, with a refractive index increment for the mono-PEG-lysozyme conjugates estimated as the weighted average of those for unconjugated lysozyme and PEG, of approximately 0.04 molecules/nm^2 and 0.01 molecules/nm^2 for bulk concentrations of 10 μmol/L and 0.1 μmol/L mono-PEG-lysozyme, respectively [2]. Fig. 1 shows the surface concentration values determined by neutron reflectivity along with those previously determined by optical reflectometry [2]. While the upper limit of the surface concentration determined by neutron reflection at 10.8 μmol/L is 25% lower than previously reported, this is still above the threshold surface concentration at which the isotherm transition was observed to occur via optical reflectometry. The smaller surface concentration measured in the current study may reflect the lower shear rates accessible in the neutron reflection flowcell than those used in the previous optical study. This would produce lower surface fluxes, which could lead to lower final surface concentrations due to the greater time allowed for structural relaxations in individual molecules as the layer is populated.

Basic layer morphology information may be obtained by comparing the projected area of an unperturbed PEG chain, πR_G^2, to the experimentally determined footprint area of the adsorbed conjugates, $1/\Gamma$: if the ratio of the projected area of the polymer to the footprint area of the conjugate is greater than one, this suggests the polymer is stretched from the surface to avoid chain overlap; if it is less than one, this suggests there is no polymer overlap. The weight-average radius of gyration R_g for the unconjugated deuterated PEG sample dissolved in aqueous solution was independently determined by small angle neutron scattering to be 3.7 nm [8]. Taking $R_g = 3.7$ nm, the area ratio $\pi R_g^2/(1/\Gamma) = 1.2$ at the higher bulk concentration. This corresponds to a mild degree of stretching of the PEG chains of the adsorbed conjugates, consistent with a layer of PEG chains in a mushroom-like, or a weakly stretched brush, regime. At the lower concentration, this comparison gives $\pi R_g^2/(1/\Gamma) = 0.7$, indicating no overlap of PEG chains.

The distribution of lysozyme and PEG between the two sublayers is consistent with the proposed transition in orientation. At the low bulk concentration, below the transition, there are nearly

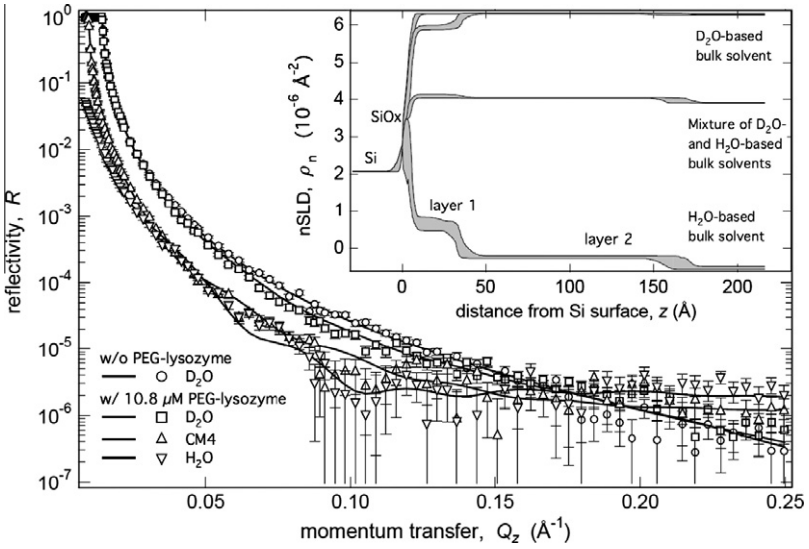

Fig. 2. Reflectivity and simultaneous best-fit for all data sets for the high-concentration (10.8 μmol/L) measurements in different contrast matching conditions with 68% error bars. Inset: 95% confidence envelopes from MC simulated scattering length density profiles.

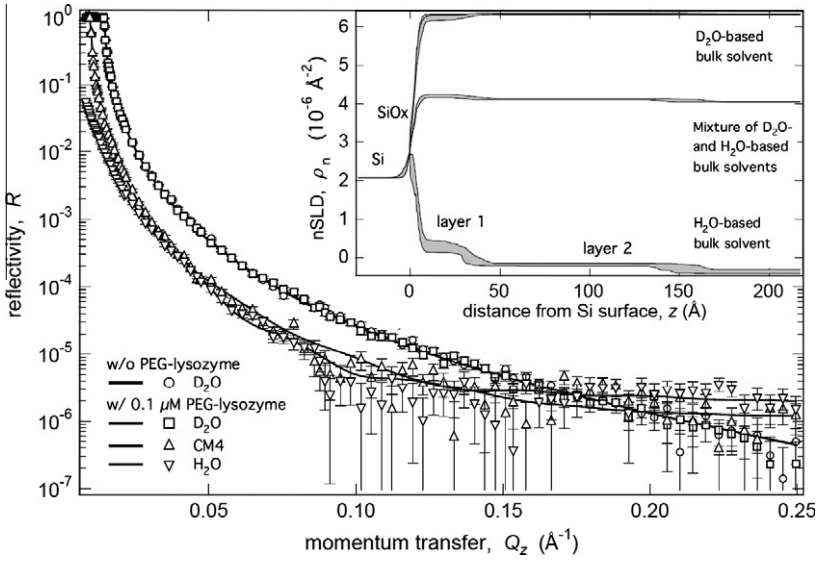

Fig. 3. Reflectivity and simultaneous best-fit for all data sets for the low-concentration (0.1 μmol/L) measurements in different contrast matching conditions with 68% error bars. Inset: 95% confidence envelopes from MC simulated scattering length density profiles.

equal volumes of lysozyme and PEG in the surface-proximal sublayer 1; the PEG-to-lysozyme volume fraction ratio is 0.066/0.058 = 1.13 in the $2.57^{+0.55}_{-0.75}$ nm thick sublayer 1. PEG and lysozyme are both present in the relatively thick ($12.1^{+0.77}_{-1.00}$ nm) sublayer 2. The PEG-to-lysozyme volume fraction ratio in sublayer 2 is 5. More than two-thirds of the lysozyme by mass resides in the surface proximal region. While we do not resolve the detailed *d*PEG density distribution within sublayer 1, the volume fractions of PEG and lysozyme in the layer are nearly equal, and the layer thickness is similar to the dimensions of lysozyme and smaller than the R_G of the free PEG. This suggests that both PEG and lysozyme have direct contact with the surface. The presence of PEG in the surface proximal region is likely promoted by the surface activity of PEG at the silica/water interface [17,18]. The occurrence of a small, but significant amount of lysozyme in sublayer 2 suggests that some of the lysozyme molecules are not directly in contact with the surface and may be anchored by their conjugated PEG chains.

The maximum dimension of a lysozyme molecule is 4.5 nm. This exceeds the ~3.0 nm sublayer 1 thickness but is well below the sublayer 2 thickness. It is conceivable that rather than some lysozyme molecules being anchored by their PEG grafts, some lysozyme molecules were adsorbed in an end-on orientation. This would contribute lysozyme mass to sublayer 2, but only to the inner portion of that layer. Model fitting suggests that this is not the case. Fitting the data to a three sublayer model, that might have captured this type of uneven distribution of lysozyme outside the surface-proximal region by further subdividing the distal region into two regions, still indicated that lysozyme was present beyond 9 nm from the surface (not shown). PEG anchorage of some of the mono-*d*PEG-lysozyme conjugates at the lower surface concentration is the most consistent interpretation of the data.

At the high concentration, 10.8 μmol/L, the overall layer thickness is $15.96^{+0.75}_{-0.86}$nm. This is somewhat more compact than the maximum dimension of mono-PEG-lysozyme in solution, esti-

Table 3
Fitted box model parameters, including sublayer thicknesses and lysozyme and *d*PEG volume fractions, from neutron reflectivity profiles of mono-*d*PEG-lysozyme adsorbed on silica at high (10.8 μmol/L) and low (0.1 μmol/L) bulk concentrations. Results represent the means of simultaneous Monte Carlo fits of the model for multiple contrast conditions. Error limits indicate upper and lower bounds at 95% confidence.

Bulk conjugate concentration (μmol/L)	10.8	0.1
Silicon oxide		
Thickness (nm)	$0.38^{+0.17}_{-0.08}$	$0.30^{+0.01}_{-0.02}$
nSLD (10^{-6} Å^{-2})	3.48 (fixed)	3.48 (fixed)
Sublayer 1		
Thickness, d_1 (nm)	$2.97^{+0.12}_{-0.14}$	$2.57^{+0.55}_{-0.75}$
Volume fraction lysozyme, $\pi_{1,\text{lysozyme}}$	$0.134^{+0.012}_{-0.011}$	$0.058^{+0.020}_{-0.020}$
Volume fraction dPEG, $\pi_{1,\text{dPEG}}$	$0.106^{+0.016}_{-0.014}$	$0.066^{+0.012}_{-0.013}$
Sublayer 2		
Thickness, d_2 (nm)	$12.99^{+0.68}_{-0.80}$	$12.10^{+0.77}_{-1.00}$
Volume fraction lysozyme, $\pi_{2,\text{lysozyme}}$	$0.000^{+0.000}_{-0.000}$	$0.004^{+0.004}_{-0.004}$
Volume fraction dPEG, $\pi_{2,\text{dPEG}}$	$0.037^{+0.002}_{-0.003}$	$0.020^{+0.003}_{-0.002}$
Global parameters		
Substrate roughness (nm)	$0.59^{+0.21}_{-0.32}$	$0.58^{+0.12}_{-0.09}$
Adsorbed layer roughness (nm)	$0.89^{+0.67}_{-0.59}$	$1.16^{+0.84}_{-0.77}$
X^2	1.94	1.85
p-value (degrees of freedom = 437)	>0.9999	>0.9999

Table 4
Computed sublayer and overall surface concentrations, Γ, of lysozyme and *d*PEG on silica at high (10.8 μmol/L) and low (0.1 μmol/L) bulk concentrations of mono-*d*PEG-lysozyme. Results represent the means derived from simultaneous Monte Carlo fits of the box model for multiple contrast conditions. Error limits indicate upper and lower bounds at 95% confidence.

Bulk Conjugate Concentration (μmol/L)	10.8	0.1
Sublayer 1 surface concentration (molecules/nm^2)		
$\Gamma_{1,\text{lysozyme}}$	$0.0285^{+0.0016}_{-0.0016}$	$0.0119^{+0.0024}_{-0.0027}$
$\Gamma_{1,\text{dPEG}}$	$0.0113^{+0.0016}_{-0.0012}$	$0.0069^{+0.0010}_{-0.0011}$
Sublayer 2 surface concentration (molecules/nm^2)		
$\Gamma_{2,\text{lysozyme}}$	$0.0000^{+0.0000}_{-0.0000}$	$0.0038^{+0.0030}_{-0.0030}$
$\Gamma_{2,\text{dPEG}}$	$0.0172^{+0.0007}_{-0.0011}$	$0.0088^{+0.0011}_{-0.0012}$
Overall surface concentration (molecules/nm^2)		
Γ_{lysozyme}	$0.0285^{+0.0016}_{-0.0016}$	$0.0157^{+0.0018}_{-0.0016}$
Γ_{dPEG}	$0.0285^{+0.0016}_{-0.0016}$	$0.0157^{+0.0018}_{-0.0016}$

mated by SANS as about 21.2 nm [8]. Lysozyme resides exclusively in the $2.97^{+0.12}_{-0.14}$ nm thick sublayer 1; the $12.99^{+0.68}_{-0.80}$ nm thick sublayer 2 contains only PEG. While there is still PEG in the proximal layer for the higher concentration experiment, the PEG-to-lysozyme volume ratio (0.106/0.134 = 0.79) is significantly lower than it was in the low concentration case. By volume, PEG was clearly the minority component in the surface proximal sublayer in the high concentration case, above the transition, while it was the majority component below the transition. Prior small angle neutron scattering measurements indicated that the radius of gyration for the PEG chain when conjugated to lysozyme is 5.14 nm [8]. The 13.0 nm sublayer 2 thickness, compared to twice this R_G (10.3 nm) is consistent with a mild stretching of conjugated PEG compared to its conformation when mono-*d*PEG-lysozyme is in solution.

4. Conclusions

Simultaneous model fitting to neutron reflectivity with three widely differing contrast matching conditions indicates that the structure of adsorbed layers of mono-PEGylated lysozyme conjugates on silica changes between low and high surface concentrations. As the surface is increasingly populated, the layer transitions from a structure at the low surface concentration where

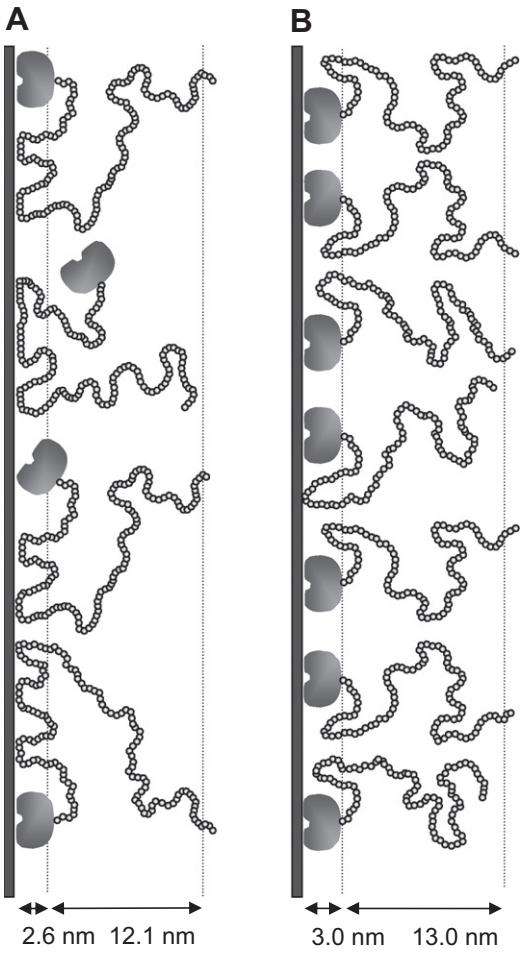

Fig. 4. Schematic illustration of the layer structure at low (A) and high (B) surface concentrations of mono-*d*PEG-lysozyme adsorbed to silica. Horizontal lines denote the edges of the regressed thicknesses of sublayers 1 and 2. The locus of PEG grafting to lysozyme is on the face opposite the active site cleft as shown.

PEG and lysozyme are relatively equally distributed in the surface proximal region and both PEG and lysozyme are present in a distal region, to a structure at high surface concentration where preferential adsorption of lysozyme forces the PEG chains away from the surface, leaving the outer region exclusively populated by PEG while the inner region is dominated by lysozyme. The key differences between the low and high surface concentration layer structures are schematically illustrated in Fig. 4.

At low surface concentration, the conjugates have a high PEG volume occupancy of the surface proximal region, with the PEG-occupied volume exceeding the lysozyme-occupied volume by 13%. Both lysozyme and PEG are present throughout a layer of overall thickness equal to $14.97^{+0.92}_{-1.25}$ nm. Most of the lysozyme resides in the surface proximal layer, but approximately 1/3 of the lysozyme mass is present at a distance from the surface that exceeds the size of the protein, indicating that some conjugates may be anchored via their PEG chains. At higher surface concentration, the data are consistent with PEG chains extending further into solution, adopting a weakly-stretched conformation preferentially anchored by lysozyme. The distal, $12.99^{+0.68}_{-0.80}$ nm thick sublayer only contains PEG, and the balance of lysozyme and PEG volume occupancy of the surface proximal sublayer, the thickness of which is comparable to the width of a lysozyme molecule, is shifted in favor of lysozyme.

This work has practical implications for PEGylated protein purification, particularly for proteins at pHs below their isoelectric

point. The different distributions of the protein and PEG portions of the conjugate at different surface concentrations suggests opportunities for the design of chromatographic separation protocols based on the primarily electrostatic nature of the lysozyme/silica interaction and the hydrogen bonding nature of the PEG/silica interaction. Added electrolytes, or H-bond altering agents such as urea or guanidinium ion may be judiciously incorporated to alter relative affinities of PEG and protein conjugate portions for the media. This also suggests that the binding mode will be coverage dependent, from a mixed electrostatic/H-bonding mode at low coverage to an electrostatic mode at high coverage, suggesting strategies for chromatographic separations run at different points on the adsorption isotherm.

Acknowledgments

This material is based on work supported by the National Science Foundation under Grant CBET 0755284. Certain commercial equipment, instruments, or materials (or suppliers, or software, etc.) are identified in this paper to foster understanding. Such identification does not imply recommendation or endorsement by the National Institute of Standards and Technology, nor does it imply that the materials or equipment identified are necessarily the best available for the purpose. This work utilized facilities supported in part by the National Science Foundation under Agreement No. DMR-0454672. The authors acknowledge Dr. Kunlun Hong at Oak Ridge National Laboratory (ORNL) for synthesis of the deuterated mPEG-PA. The synthesis was conducted at the Center for Nanophase Materials Sciences (CNMS), which is sponsored at ORNL by the Office of Basic Energy Sciences, US Department of Energy through the CNMS user program (user Proposal Number: CNMS2009-212).

References

[1] C. Pinholt, J.T. Bukrinski, S. Hostrup, S. Frøkjaer, W. Norde, L. Jørgensen, European Journal of Pharmaceutics and Biopharmaceutics 77 (2011) 139–147.
[2] S.M. Daly, T.M. Przybycien, R.D. Tilton, Langmuir 21 (2005) 1328–1337.
[3] L. Haggerty, A.M. Lenhoff, Biophysical Journal 64 (1993) 886–895.
[4] S.M. Daly, T.M. Przybycien, R.D. Tilton, Langmuir 19 (2003) 3848–3857.
[5] J.L. Robeson, R.D. Tilton, Langmuir 12 (1996) 6104–6113.
[6] T.J. Su, J.R. Lu, R.K. Thomas, Z.F. Cui, J. Penfold, Journal of Colloid and Interface Science 203 (1998) 419–429.
[7] S.S. Pai, T.M. Przybycien, R.D. Tilton, Langmuir 26 (2010) 18231–18238.
[8] S.S. Pai, B. Hammouda, K. Hong, D.C. Pozzo, T.M. Przybycien, R.D. Tilton, Bioconjugate Chemistry 22 (2011) 2317–2323.
[9] J.A. Dura, D.J. Pierce, C.F. Majkrzak, N.C. Maliszewskyj, D.J. McGillivray, M. Lösche, K.V. O'Donovan, M. Mihailescu, U. Perez-Salas, D.L. Worcester, S.H. White, Review of Scientific Instruments 77 (2006) 1–11.
[10] C.F. Majkrzak, N.F. Berk, S. Krueger, J.A. Dura, M. Tarek, D. Tobias, V. Silin, C.W. Meuse, J. Woodward, A.L. Plant, Biophysical Journal 79 (2000) 3330–3340.
[11] J.F. Ankner, C.F. Majkrzak, in: SPIE Conference Proceedings, vol. 1738, 1992, pp. 260–266.
[12] S.J. Perkins, European Journal of Biochemistry 157 (1986) 169–180.
[13] V.F. Sears, Neutron News 3 (1992) 26–37.
[14] P.A. Kienzle, M. Douchet, D.J. McGillivray, K.V. O'Donovan, N.F. Berk, C.F. Majkrzak, 2000–2009. <http://www.ncnr.nist.gov/reflpak/garefl.html>.
[15] F. Heinrich, T. Ng, D.J. Vanderah, P. Shekhar, M. Mihailescu, H. Nanda, M. Lösche, Langmuir 25 (2009) 4219–4229.
[16] H.M. Berman, J. Westbrook, Z. Feng, G. Gilliland, T.N. Bhat, H. Weissig, I.N. Shindyalov, P.E. Bourne, Nucleic Acids Research 28 (2000) 235–242.
[17] Z. Fu, M.M. Santore, Langmuir 13 (1997) 5779–5781.
[18] B.R. Postmus, F.A.M. Leermakers, M.A. Cohen, Stuart, Langmuir 24 (2008) 1930–1942.